Journal of Applied Polymer Science

The effect of TiO_2 nanoparticles on the properties of sulfonated block copolymers

Ariangelís Ortiz-Negrón, David Suleiman
Chemical Engineering Department, University of Puerto Rico, Mayagüez, Puerto Rico, 00681-9000
Correspondence to: D. Suleiman (E-mail: David.Suleiman@upr.edu)

ABSTRACT: Block copolymers composed of styrene and different elastomeric blocks were sulfonated to high ion exchange capacities (IECs). Titanium dioxide (TiO_2) nanoparticles were added to these polymers to improve their mechanical and thermal stabilities, while influencing their transport properties for direct methanol fuel cell (DMFC) applications. Materials properties as proton exchange membranes (PEMs) were analyzed using: FT-IR, water absorption, thermogravimetric analysis (TGA), differential scanning calorimetry (DSC), IEC, methanol permeability, and proton conductivity studies. Although there was no effect of TiO_2 nanoparticles on the thermal stability of the membranes, significant changes were observed in the mechanical properties of both sulfonated block copolymers studied. Water absorption increased at low TiO_2 content, but was then reduced with the incorporation of more nanoparticles. To enhance the interaction between the inorganic fillers and the polymers, sulfonic and amino groups were attached to the surface of the titania nanoparticles. The effect of sulfonated nanoparticles on the properties of the materials was more significant than the effect of the amino functionalized nanoparticles on all the properties evaluated, suggesting enhanced chemical interactions with the ionic domains of the polymer membranes. © 2015 Wiley Periodicals, Inc. J. Appl. Polym. Sci. **2015**, *132*, 42651.

KEYWORDS: batteries and fuel cells; composites; conducting polymers; copolymers; nanoparticles; nanowires and nanocrystals

Received 31 January 2015; accepted 24 June 2015
DOI: 10.1002/app.42651

INTRODUCTION

Organic-inorganic polymer nanocomposite membranes (PNM) have been studied for direct methanol fuel cell (DMFC) applications since they could better withstand normal operating conditions, without sacrificing their properties, as opposed to common proton exchange membranes (PEM). The organic-inorganic fillers often provide the membrane with improved mechanical and thermal stability,[1] while enhancing the water retention in the membranes. Water can be critical in sulfonated polymers, since water bound to ionic domains plays a critical role in the transport of protons through the membrane.[2,3] In addition, the presence of the inorganic fillers often decreases the free-volume, reducing the fuel crossover through the membrane.[4] The most common inorganic additives are metal oxides (SiO_2, TiO_2, ZrO_2). These fillers have been applied in the modification of materials from the state-of-the-art PEM, the perfluorinated sulfonated Nafion®,[5,6] to many other PEMs with unique chemical functionalities and morphologies (e.g., PEEK,[7,8] poly ether sulfone[9] etc.) with different and unique results, based on chemical interactions and changes in the resulting morphology of the ionic polymers (ionomers).

Block copolymers have advantages such as low cost, good processability, ease of functionalization, and the combination of properties provided by the difference in nature of the hydrophobic and hydrophilic domains.[10] In these materials, the elastomeric block provides good flexibility and helps blocking the transport of fuel and electrons, while the aromatic block provides the pathway for the transport of protons after being functionalized with an ionic group (i.e., sulfonation). Sulfonation of these polymers provides the membrane with good transport properties, by the absorption of water and the subsequent formation of hydrogen bonds. The blocks in the polymer arrange in different manners, forming micro-domains due to the difference in properties and affinity among them. The arrangement of the micro-domains and the morphology vary with elastomeric block and degree of sulfonation, which affects the resulting thermal, mechanical, and transport behavior of the membranes. Aviles-Barreto and coworkers[11] studied poly(styrene-isobutylene-styrene) (SIBS) at different sulfonation levels using small angle X-ray scattering (SAXS). The results showed that morphology changed with sulfonation level, and that these differences affected the proton conductivity and methanol permeation of the membranes. Mauritz *et al.*[12] studied the effect of sulfonation on the morphology of poly(styrene-ethylene/butylene-styrene) (SEBS) and determined that the morphology changed from hexagonally packed cylinders, in the pristine

unmodified material, to lamellar when sulfonated, even at low degrees of sulfonation. At fuel cell operating temperatures (70–120°C), these membranes tend to dehydrate and lose mechanical stability. Thus promoting the use of organic-inorganic PNM to overcome this limitation.

Among the metal oxide fillers, titanium dioxide has gained attention in different applications due to its good thermal, mechanical, and optical properties, low cost, chemical stability, and non-toxicity.[13] There are three principal crystal phases in TiO_2; anatase, rutile, and brookite, being rutile the most stable and anatase the crystalline phase most commonly found in the literature.[4,14,15] Different nanostructures can be obtained with titanium dioxide; nanoparticles, nanowires, nanotubes, and nanofibers.[16] Studies suggest that the nanostructure often affects the properties and performance of the material in different applications.[15] Matos *et al.* studied the effect of three different structures (nanotubes, near-spherical particles, and mesoporous high surface area particles) of TiO_2 fillers on the properties of Nafion®, and found-out that the highest current densities and proton conductivities were obtained with nanotubes, when compared with the other structures studied.[17]

The biggest challenge found when synthesizing organic-inorganic PNM arises when agglomerations are formed and there are no interactions with the polymeric matrix.[18] Another drawback of the incorporation of inorganic fillers is the possible reduction in proton conductivity.[19] To reduce these agglomerations and create affinity with organic solvents, surface functionalization of the inorganic nanoparticles has been studied. Some functionalizations found in the literature include sulfonation and amine tailoring. Xu *et al.* studied the effect of titanium dioxide and sulfonated titanium dioxide nanoparticles in the methanol permeability and proton conductivity of sulfonated PEEK.[19] Their results showed that an increment in the amount of nanoparticles present in the membrane reduced the methanol permeability and increased the selectivity. The effect of the nanoparticles was still more significant when they were functionalized. The effect of sulfonated TiO_2 nanoparticles on Nafion® membranes was analyzed by Jun *et al.*[18] The proton conductivity of the TiO_2 nanotubes increased by two orders of magnitude after sulfonation, while the effect on the membranes was more significant at low relative humidity. Amino functionalized titania nanotubes were incorporated into Nafion® and enhanced proton conductivities were obtained at low filler contents (7 wt %). However, an increment in the concentration of these materials reduced the conductivity, which, as explained by the authors, was probably caused by the blockage of proton transport sites.[20] The effect of enhanced conductivity was accompanied by an increment in water absorption when comparing functionalized and non-functionalized titania. Amino groups could work as water in proton conduction, because they can form NH_3^+ and become proton donors, helping in the transport of protons through the membrane.

Given the good results obtained by some groups in applying PNMs as PEMs, and the recurring need to develop efficient and economically viable energy sources, this research work focused on the modification of two inexpensive sulfonated block copolymers with different loadings of TiO_2 nanoparticles and with functionalized nanoparticles to develop PEMs for DMFC applications. The block copolymers studied were sulfonated SIBS and sulfonated SEBS. Different characterization techniques such as: elemental analysis (EA), Fourier-transform infrared spectroscopy (FT-IR), Raman spectroscopy, thermogravimetric analysis (TGA), water absorption, ion exchange capacity (IEC), atomic force microscopy (AFM), tensional static measurements, SAXS, wide angle X-ray scattering (WAXS), methanol permeability, and proton conductivity were performed to determine the effect of the modifications on the PNMs chemical, thermal, mechanical, and transport properties.

EXPERIMENTAL

Materials

SIBS ($M_n = 65{,}000$, 30% polystyrene) was obtained from Kaneka®, while SEBS G1652 ($M_n = 26{,}000$ as determined by GPC with polystyrene standards, 30% polystyrene) was obtained from Kraton Polymers. Sulfuric acid (95–98%), acetic anhydride (99+%), hexyl alcohol (98%), anatase titanium dioxide (<25 nm crystals, 99.7%), titanium dioxide nanowires ($d \times L$, 10 nm×10 μm), (3-aminopropyl)trimethoxysilane (APTMS) (97%), triethylamine (TEA) (≧99%), (3-mercaptopropyl)trimethoxysilane (MPTMS) (95%), and hydrogen peroxide (35 wt % in H_2O), were obtained from Sigma-Aldrich. Methanol (99.9%), methylene chloride (99.8%), and toluene (Optima, 99.8%) were purchased from Fisher Scientific. All chemicals were used without further purification.

Experimental Overview

Two different polymers were selected to study differences in elastomeric blocks given that these polymers had the same concentration of polystyrene and a previous study on SIBS membranes[21] suggested that the effect of molecular weight on DMFC transport properties was not very significant. The next variable studied was the degree of sulfonation, although for both polymers the degrees of sulfonation were different, the idea was to obtain similar sulfonation percents for both polymers. Next, the intention was to study two different loadings of titania nanoparticles to determine the effect of concentration. However, due to the formation of two phases upon the incorporation of unfunctionalized titania nanoparticles, two different functionalizations at the lowest loading were studied. After completing the analysis of the nanoparticle loading and functionalization, one membrane was prepared with titania nanowires for comparison purposes.

Sulfonation

Membranes were prepared with two different acetyl sulfate to polymer molar ratios (3 : 1 and 5 : 1), for both SEBS and SIBS (Figure 1), to obtain different sulfonation levels. The sulfonation procedure is described in detail elsewhere.[22] Briefly, 30 grams of polymer were dissolved in 300 mL of methylene chloride on a round three-neck reactor. On an Erlenmeyer in an ice bath the sulfonating agent was prepared by adding specific amounts of methylene chloride, acetic anhydride, and sulfuric acid depending on the desired molar ratio. After 24 h of continuous stirring, the reaction is stopped with the addition of 200 mL of methanol.

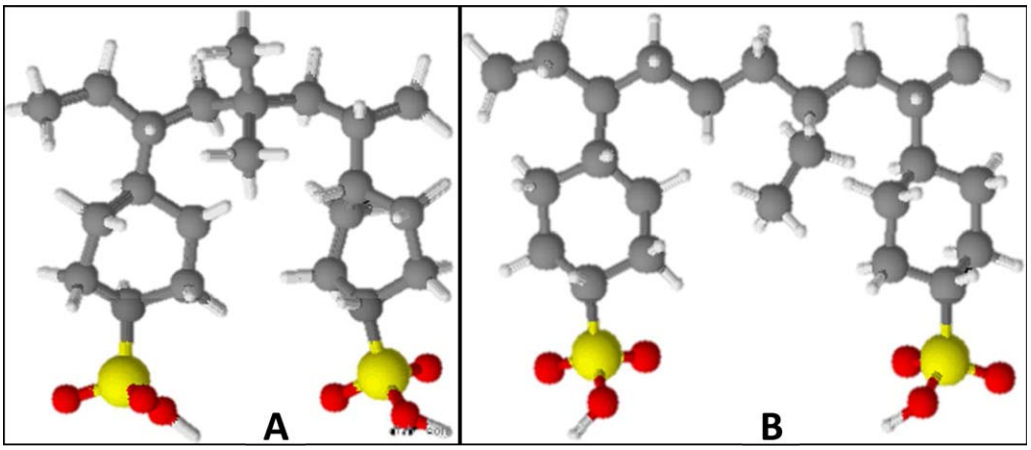

Figure 1. Structures of (A) poly(styrene-isobutylene-styrene) (SIBS) and (B) poly(styrene-ethylene/butylene-styrene) (SEBS). [Color figure can be viewed in the online issue, which is available at wileyonlinelibrary.com.]

Titania Functionalization

Due to the high density of the titania nanoparticles, poor interaction of these nanoparticles with the polymer can be obtained and has been observed on the literature.[23] A new approach, based on the surface modification of the nanoparticles and their incorporation on the polymer matrix, began to be applied to overcome this difficulty.

For the sulfonation of the nanoparticles 9.3 mL of MPTMS were added, dropwise, to a partial suspension of 2 g of TiO_2 in 53 mL of toluene and some drops of TEA.[18] The reaction took place for 24 h at 110°C, under reflux conditions. The resulting material was oxidized to sulfonic groups with the addition of 30 mL of hydrogen peroxide (35 wt % solution in water) for 24 h. For the oxidation reaction, the reactor had to be placed on an ice bath to maintain a low temperature, given that the reaction is highly exothermic.

The amino functionalization was achieved by the addition of a solution of 0.5 g of APTMS in 10 mL of toluene to a partial dispersion of 0.5 g of TiO_2 nanoparticles in 25 mL toluene (containing some drops of TEA). This reaction took place at ambient temperature, under nitrogen atmosphere, for 24 h.[20] Before the addition of APTMS, the system was first evacuated and then filled with nitrogen.

The materials obtained from both functionalizations were washed in toluene, ethanol, a 50% (v/v) ethanol in de-ionized water solution, and de-ionized water, then centrifuged, and dried in an oven at 60°C for at least 24 h.

Incorporation of Titania Nanoparticles

Two different loadings, 1 and 3 wt %, of TiO_2 nanoparticles were added to the polymer solution. These loadings were selected based on the commonly used values found in the literature.[4,20,24] After ultrasonication on an Aquasonic 75HT ultrasonic bath for at least one hour in a toluene and hexanol solution, the dispersion was added to the polymer solution and dispersed again before membrane casting. For the incorporation of functionalized nanoparticles only the 1 wt % loading was used.

Membrane Casting

After sulfonation and titania incorporation the membranes were prepared using the solvent casting procedure at ambient temperature. A 5–10% (w/v) solution of the polymer in toluene (85%) and hexyl alcohol (15%) was prepared and then added to teflon petri dishes until the solvent was completely evaporated. Before characterization, membranes were dried in an oven at 60°C for 24 h to remove any remaining solvent. Thickness of the membranes varied with the concentration of the polymer solution and the amount of solution added to the petri dish. However, for transport experiments (proton conductivity and methanol permeability) the thickness of the membranes was measured and taken into consideration in the calculations.

Chemical, thermal, and mechanical properties of the PNMs were characterized to have a better understanding of the effects caused by the modifications. The chemical functionalization of the nanoparticles was confirmed employing FT-IR, DSC, and TGA techniques.

Membrane Characterization

After membrane casting, EA was conducted by Atlantic Microlabs, in Norcross, Georgia. In this experiment, membrane samples were analyzed for carbon, hydrogen, oxygen, and sulfur content. With the relative amounts obtained and a material balance calculation, the sulfonation level was determined as the percent of sulfonated aromatic rings in polystyrene.

Chemical characterization of the membranes was performed with FT-IR and Raman spectroscopy. FT-IR experiments were conducted on a Bruker Alpha Platinum ATR spectrometer with a diamond crystal. 200 scans were performed for each sample at a resolution of 6 cm^{-1} in the wavenumber range of 4,000–400 cm^{-1}. Raman spectra were acquired using a confocal Raman microscope XploRa (Horiba Scientific) with a laser wavelength of 638 nm, using a 10× objective.

To determine the stability of the membranes at the operating temperature of the fuel cell, and the effect of sulfonation and incorporation of the titania nanoparticles on the thermal stability of the polymer chain, TGA was conducted on the membranes. Samples of 5–10 mg were used for this experiment.

Measurements were conducted on a TGA/SDTA 851 (Mettler Toledo) from 25 to 800°C at 10°C/min under nitrogen atmosphere.

Thermal transitions in the materials were studied using DSC in a TA Instruments Q 2000 DSC. Samples with masses ranging from 10 to 15 mg were cooled down to −80°C, at a rate of 5°C/min, and then heated up to 350°C, at a rate of 10°C/min, under nitrogen atmosphere, with a nitrogen flowrate 50 mL/min.

Stress-strain measurements were performed with an Anton Paar Rheometer MCR 302 equipped with an extensional rheology system, SER, and a convective heating device (CTD 450). Measurements were carried out at ambient temperature at a strain rate of 0.1 min^{-1}.

SAXS and WAXS experiments were conducted on an Anton Paar SAXSpace equipment. Samples were exposed for 30 s and 7 mins for SAXS and WAXS, respectively. Measurements were made normal to the plane of the membrane.

Phase images were obtained with an AFM 5500 Scanning Probe Microscope (Agilent Technologies) in AC mode and at ambient conditions.

For water absorption measurements the membranes were first dried in an oven at 60°C for 24 h. Then their dry masses were recorded. Samples were then immersed on de-ionized water. The mass of the samples was monitored along time until equilibrium was achieved.[25–27]

IECs were obtained taking a known mass of membrane and submerging it in a 1*M* solution of NaCl for 24 h. After this period of time, membranes were carefully removed from the vial and the remaining solution was titrated with NaOH 0.01*M* to determine IEC. IECs were calculated from the substituted moles of Na^+ divided by the mass of the dry polymer.

Membrane Transport Properties

Methanol permeability measurements were conducted by placing the membrane in a liquid diffusion cell with de-ionized water on one compartment and a 2*M* methanol solution on the other. The concentration of methanol on the compartment that initially contained water was recorded during 2 h, using a Shimadzu gas chromatographer, equipped with a packed column (Porapack T) and a thermal conductivity detector (TCD). Membrane's thickness, cross-sectional area, and the volume of the cell must be well-known for the permeability calculations.

Measurements of impedance spectroscopy were carried out in an 850e Fuel Cell Test Station (Scribner and Associates) at 100% relative humidity and 80°C. Membranes were fully hydrated before the experiments.

All measurements were made with three replicates and the error bars correspond to the standard deviation of the measurements.

Membrane selectivities were calculated as the ratio of the proton conductivity to the methanol permeability. The selectivity was then normalized with respect to the state-of-the-art PEM, Nafion®. The standard deviation, represented by the error bars, was obtained using propagation of error calculations.

RESULTS AND DISCUSSION

Elemental Analysis

With the results obtained from the EA, the percent of sulfonated aromatic rings in styrene was calculated. Two different molar ratios of sulfonating agent to polymer were used and the results obtained were as follows: for a ratio of 3 : 1, SEBS was sulfonated in 84.1% and SIBS in 73.9%, while for the 5 : 1 sulfonation the values are, 92.7% and 82.3%, for SEBS and SIBS, respectively. For both polymers the sulfonation reaction is mass transfer limited, since as the reaction progresses the sulfonating agent has to reach available aromatic rings that might not be so easily accessible. Therefore, an excess of the sulfonating agent was always used and the reaction took place for 24 h to achieve the highest possible sulfonation and to have a homogeneous distribution of the sulfonic groups on the polymer. These results suggest that there is a greater steric impediment, maybe due to the arrangement of the elastomeric and ionic blocks in SIBS, that limits the degree of sulfonation obtained, given that for both polymers the same proportions of sulfonating agent to polymer were used, and the reactions were conducted for the same amount of time (24 h).

Titania Functionalization: Chemical and Thermal Characterization

After functionalization, titania nanoparticles were characterized by different methods to qualitatively determine the presence of the new functional groups and their effects on the properties of the material. First of all, the broad band below 850 cm^{-1} is characteristic of the Ti—O bond. FT-IR spectra in Figure 2(A) show the presence of new functional groups, for the amino and sulfonic acid functionalized nanoparticles, when compared to the unmodified particles. Bands characteristic of S—O bonds[28] are present between 1,200 and 1,000 cm^{-1}. For the amino functionalized nanoparticles the intensity of the bands is low however when compared with the spectrum for the functionalizing agent (3-aminopropyl) trimethoxysilane (APTMS) there are bands that are representative of this compound at around 2,900 cm^{-1} that are present in the spectrum of the nanoparticles. A possible explanation for the low intensity could be that the amino groups have a strong interaction among themselves and there are a few functional groups that can be detected on the exposed surface.

Figure 2(B) shows that titania nanoparticles have high thermal stability. Mass losses at temperatures below 200°C are attributed to water and/or solvent evaporation. For the pristine material, there were no other mass losses. Functionalization causes new degradations on the materials, due to the presence of new functional groups. In the sulfonated material the degradation of the sulfonic groups occurs at around 350°C, and the other mass loss could be attributed to the degradation of the silanol groups in the sulfonating agent. In the amino modified material the loss of the silanol groups is also present and there is a mass loss at higher temperatures that could be attributed to the amino groups.

In the DSC curves in Figure 2(C), the transition temperatures for the nanoparticles can be observed. For the pristine material there are transitions at 146 and 181°C. When sulfonated only

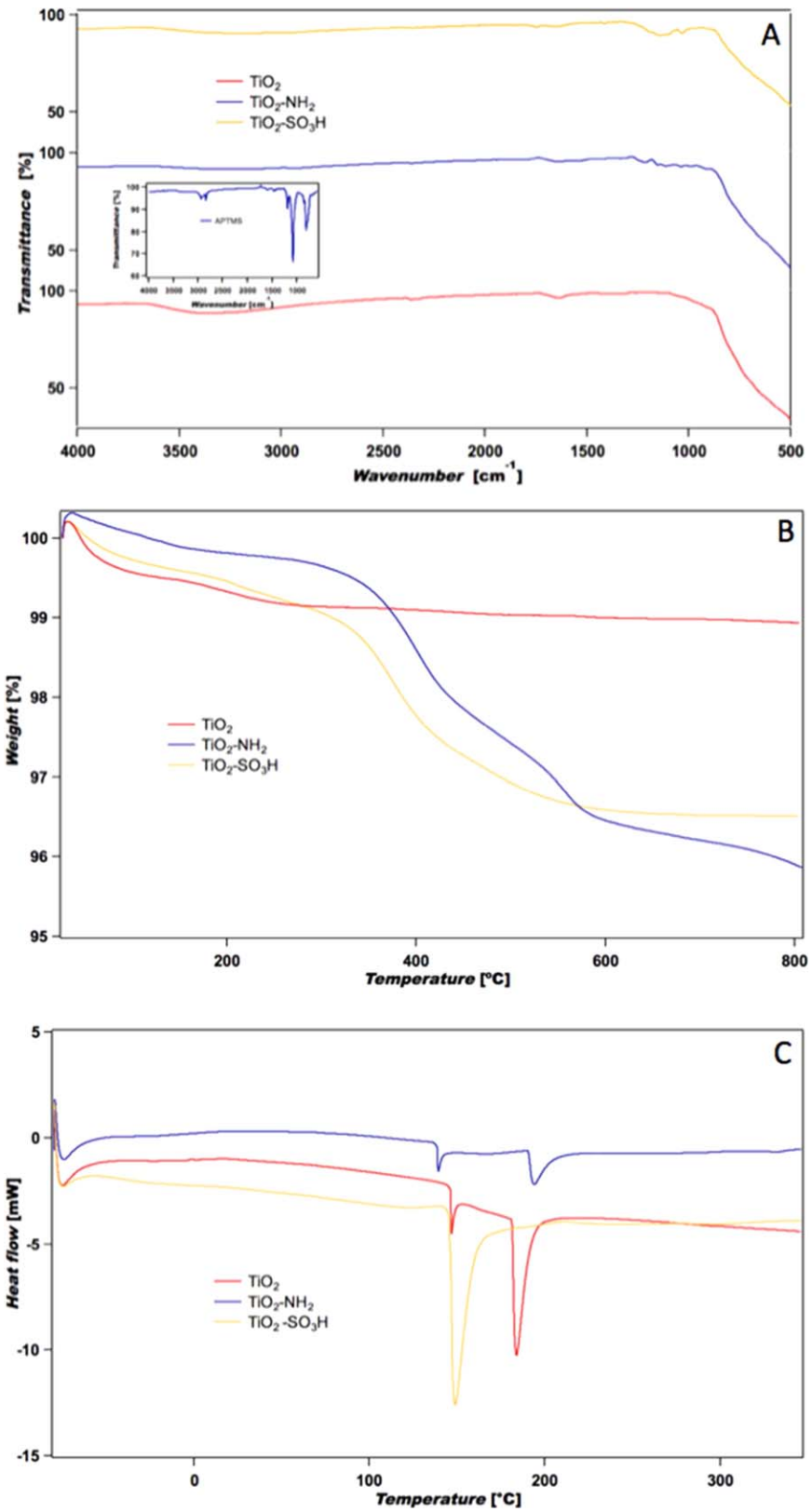

Figure 2. Functionalized titanium dioxide (A) FT-IR spectra, (B) thermogravimetric, and (C) DSC curves. [Color figure can be viewed in the online issue, which is available at wileyonlinelibrary.com.]

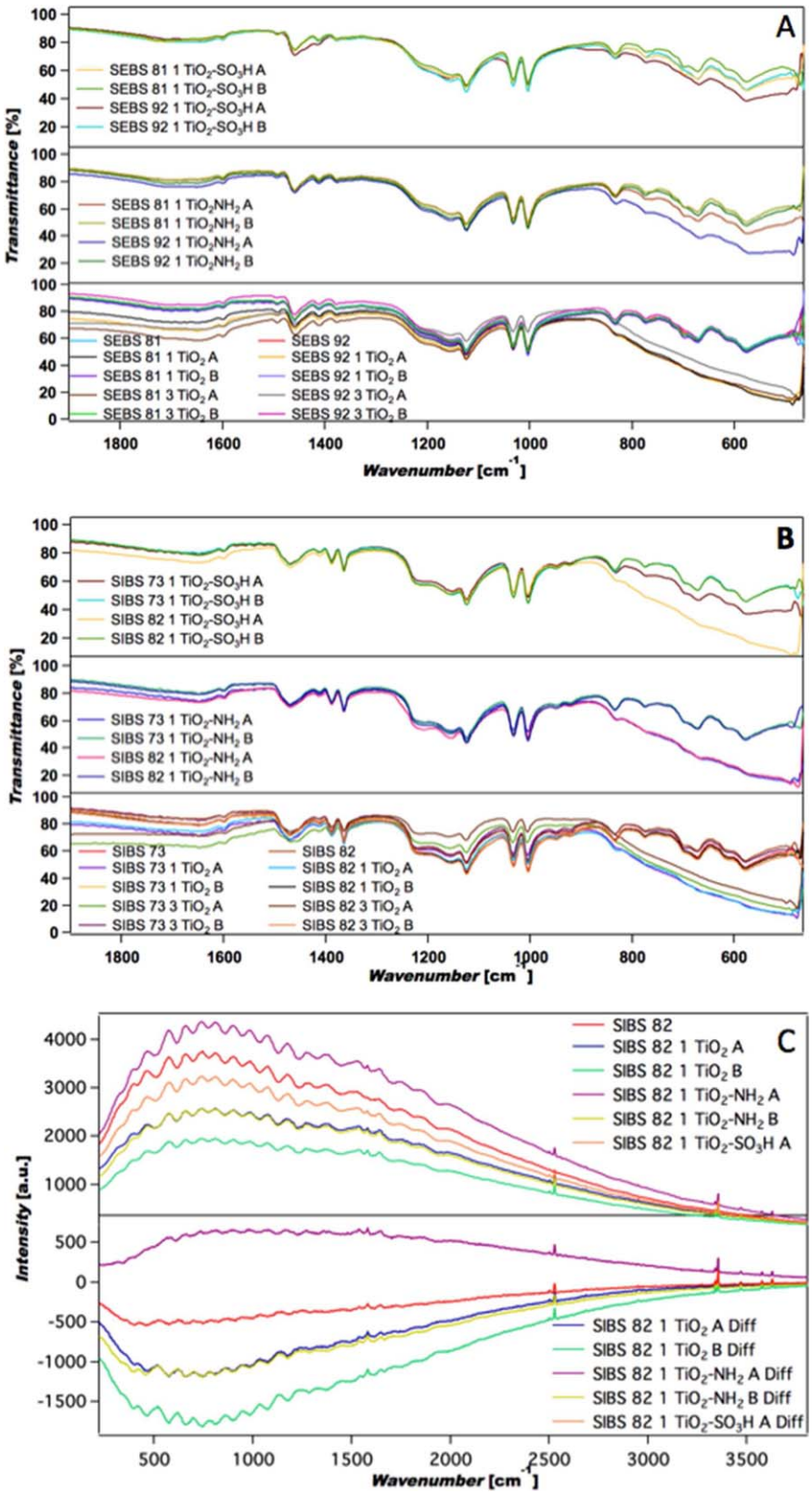

Figure 3. FT-IR spectra: Effect of titania nanoparticles on (A) SEBS and (B) SIBS, and (C) Raman spectra for SIBS 82. [Color figure can be viewed in the online issue, which is available at wileyonlinelibrary.com.]

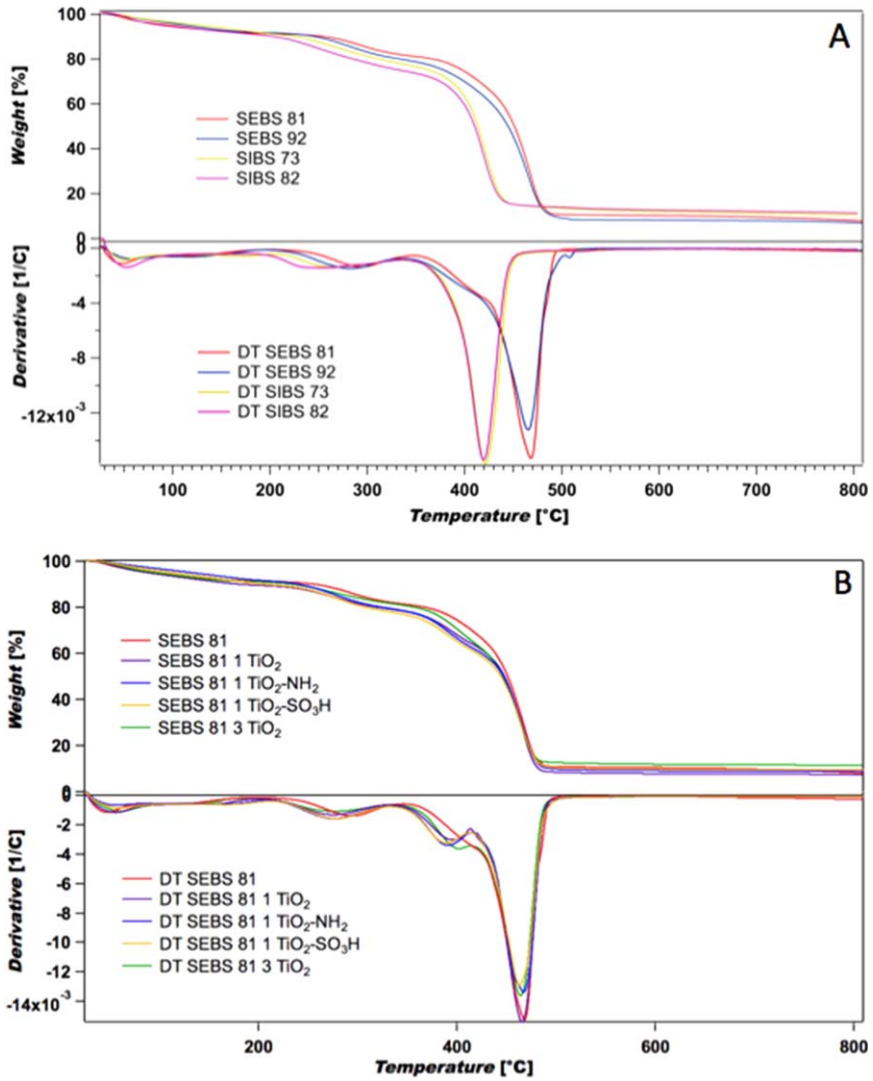

Figure 4. Thermogravimetric curves: (A) Difference among elastomers and (B) Thermogravimetric curves: Effect of titania nanoparticle loading. [Color figure can be viewed in the online issue, which is available at wileyonlinelibrary.com.]

one transition at around 146°C is observed. And finally, for the amino functionalized particles there are two transitions, but the temperatures are slightly different (138 and 190°C). With these differences it can be concluded that particles were successfully functionalized.

From now on, samples will be identified with the initials of the polymer, followed by the sulfonation percent of the membrane, then the loading of particles, and finally the particle functionalization. For example, SEBS 81 1 TiO_2-SO_3H, corresponds to SEBS with 81% sulfonation (of available polystyrene), with 1 wt % TiO_2 nanoparticles functionalized with sulfonic groups.

Fourier Transform Infrared and Raman Spectroscopy

FT-IR and Raman spectroscopy were used to qualitatively determine the effect of sulfonation and the incorporation of different loadings and functionalizations of titania nanoparticles. From the FT-IR spectra, the presence of the sulfonic groups in the polymer membranes, and the presence and interactions of the nanoparticles could be determined.[21] The broad and intense band at wavenumbers below 850 cm^{-1} [Figure 3(A,B)] confirms the presence of the nanoparticles on the membranes as stated in Figure 2(A). However, no interactions can be observed, given that there is no shift in energy for any of the bands that characterize the sulfonated polymers. A slight reduction in the intensity of the bands between 1,200 and 1,000 cm^{-1} is observed when the highest loading is incorporated (3%). In previous studies it has been suggested that there could be interaction between the nanoparticles and a specific group in the membrane if there is a reduction in the intensity of a band.[19]

What can be observed is that there is a better distribution of particles on the membranes when functionalized nanoparticles are incorporated. In this case, the spectra for the top (B) and bottom (A) parts of the membrane are very similar, and the band characteristic of Ti—O bond (800–400 cm^{-1}) has lower intensity, suggesting that particles are not agglomerated on the surface and are well distributed on the polymer matrix. A

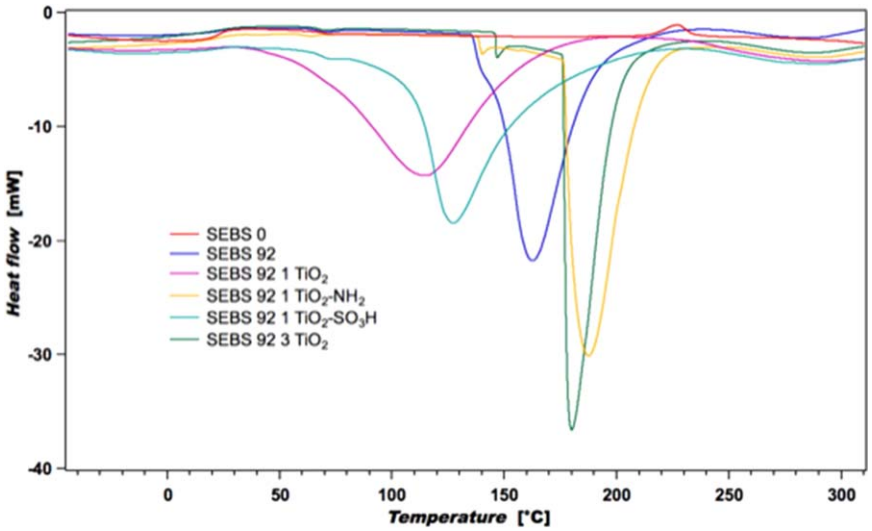

Figure 5. DSC curves SEBS 92: Effect of titanium dioxide loading and functionalizations. [Color figure can be viewed in the online issue, which is available at wileyonlinelibrary.com.]

difference between SIBS and SEBS can be observed when comparing Figure 3(A,B). The distribution of functionalized nanoparticles appears to be better on SEBS than on SIBS, suggesting better interaction of the particles with this polymer.

In Figure 3(C) the Raman spectra for SIBS 82 with the functionalized and unfuctionalized particles at 1% loading are presented. It can be seen that there are no significant differences between the spectra of the membranes with functionalized and unfunctionalized titania nanoparticles. After plotting difference spectra bands characteristic of the membranes with particles are observed. Even after functionalization the bands did no change in wavenumber, suggesting there is no difference in the chemical interaction between the particles and the polymer.

Thermogravimetric Analysis

After sulfonation the degradation temperature of the polymer increases by 15–20°C.[29] Additional degradations are observed and attributed to the loss of water and other solvents up to 200°C, and to the degradation of the sulfonic groups around 350°C. On Figure 4(A) the large difference between the degradation temperature of SIBS and SEBS can be observed. Although both polymers are similar in chemical nature and composition, the degradation temperature for SEBS is almost 50°C higher than the backbone degradation of SIBS. This difference is maintained with the incorporation of the functionalized and unfunctionalized fillers. It is observed that there is no significant effect with the addition of TiO_2 nanoparticles, regardless of the loading [Figure 4(B)]. These results could be explained by the low concentration of particles on the polymer or the absence of polymer–nanoparticle interaction. Another observation is that because sulfonation levels are similar, the difference in mass loss due to the sulfonic groups is not significant. Finally, it can be observed on Figure 4(B) that the incorporation of the functionalized particles did not enhance the thermal stability of the sulfonated polymer. It is important, however, to emphasize that the incorporation of nanoparticles did not have a negative effect on the degradation temperature of the polymers, due to the good thermal stability observed in Figure 2(B), thus maintaining membranes stability. Similar results are obtained with SIBS. It has been demonstrated that membranes are thermogravimetrically stable in the range of operation of fuel cells.

Differential Scanning Calorimetry

On Figure 5 a small exothermic transition on pristine SEBS is observed. After sulfonation, a new endothermic transition appears. Therefore, the new transition is attributed to a transition due to the sulfonic group. In Figure 2(C) the transition temperatures of the functionalized and unfunctionalized titania nanoparticles are observed, when incorporated on the membranes these transitions can also be observed (Figure 5), confirming their presence on the membrane. The incorporation of nanoparticles into the sulfonated polymer changes the temperature and energy of the endothermic transition of the sulfonic group. Changes in the temperature and energy of the endothermic transition of the sulfonic group have been observed by Unnikrishnan *et al.*[4] with other sulfonated polymer (sulfonated polysulfone), suggesting that above the polymers T_g, the nanoparticles fill the free-volume changing the movement of the segments. Both SEBS and SIBS show small relaxation temperatures below 100°C,[30] that could support the effect of the nanoparticles on the endothermic transition of the sulfonic group. Table I summarizes the changes in the endothermic temperature and the energy associated with this transition. Changes are unique for each: polymer, sulfonation level, type of functionalized nanoparticle, and loading. However, it can be seen that for each polymer, the higher the sulfonation percent the higher the energy of the transition. With the incorporation of nanoparticles the main effect is to increase the energy needed for the transition and to broaden the range of temperature in which the transition occurs, except for the amino functionalization. In this case, for both polymers and sulfonation

Table I. DSC Energy and Temperature of Transition

Membrane	Onset temperature (°C)	Peak temperature (°C)	Energy (J/g)
SIBS 73	174.0	174.0	253.1
SIBS 73 1 TiO_2	139.0	164.2	237.6
SIBS 73 1 TiO_2-NH_2	175.7	180.9	220.5
SIBS 73 1 TiO_2-SO_3H	139.4	139.4	283.8
SIBS 73 3 TiO_2	104.6	131.4	253.2
SIBS 82	149.7	166.7	264.8
SIBS 82 1 TiO_2	180.9	180.9	245.3
SIBS 82 1 TiO_2-NH_2	176.3	181.1	245.1
SIBS 82 1 TiO_2-SO_3H	182.2	184.5	229.2
SIBS 82 3 TiO_2	129.4	140.0	275
SEBS 81	185.4	185.4	252.1
SEBS 81 1 TiO_2	148.9	173.5	258.9
SEBS 81 1 TiO_2-NH_2	160.2	165.3	227.2
SEBS 81 1 TiO_2-SO_3H	119.2	147.1	249.9
SEBS 81 3 TiO_2	160.7	168.1	285.5
SEBS 92	145.4	162.8	306.7
SEBS 92 1 TiO_2	63.4	115.6	411.5
SEBS 92 1 TiO_2-NH_2	176.5	186.7	282.4
SEBS 92 1 TiO_2-SO_3H	109.3	126.9	320.2
SEBS 92 3 TiO_2	176.1	179.5	254.4

levels, the energy required for the transition was reduced making it easier to occur.

Mechanical Properties

Tensional static measurements were performed on samples at ambient temperature. Figure 6 depicts the stress versus strain plot for SIBS. The maximum elongation and stress was always obtained with the sulfonated materials without nanoparticles. Upon the incorporation of functionalized nanoparticles the membranes tend to break easily. Therefore, the membranes achieve a lower elongation and the ultimate tensile stress is significantly lower when compared to the sulfonated membrane. The reduction in elongation and stress is more significant for SEBS than for SIBS, as observed in Table II. On the other hand, after calculating the Young's (elastic) modulus, it can be observed that the difference is not as significant for most cases. A possible explanation for the changes in the mechanical properties of the PNMs is that the particles are in some instances dispersed on the elastomeric matrix, reducing its capacity to resist elongational deformation given that the elongational

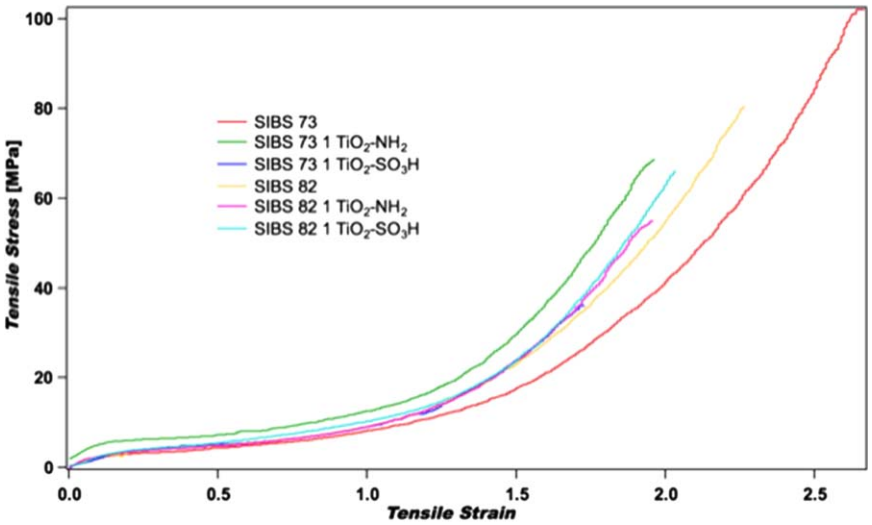

Figure 6. Stress-Strain curve for SIBS membranes: Effect of functionalized nanoparticles. [Color figure can be viewed in the online issue, which is available at wileyonlinelibrary.com.]

Table II. Mechanical Properties Summary

Sample	Elongation at break	Ultimate tensile stress (MPa)	Young's Modulus (MPa)
SIBS 73	2.6 ± 0.3	105 ± 31	25 ± 3
SIBS 73 1 TiO_2-NH_2	1.97 ± 0.01	68.5 ± 0.3	31 ± 10
SIBS 73 1 TiO_2-SO_3H	1.9 ± 0.3	47 ± 15	24 ± 9
SIBS 82	2.5 ± 0.3	96 ± 45	22 ± 3
SIBS 82 1 TiO_2-NH_2	2.0 ± 0.1	58 ± 3	30 ± 1
SIBS 82 1 TiO_2-SO_3H	1.9 ± 0.3	48 ± 38	32 ± 16
SEBS 81	3.9 ± 0.2	284 ± 73	28 ± 19
SEBS 81 1 TiO_2-NH_2	1.6 ± 0.2	17 ± 3	35 ± 10
SEBS 81 1 TiO_2-SO_3H	1.4 ± 0.5	13 ± 10	25 ± 3
SEBS 92	3.8 ± 0.2	372 ± 159	41 ± 3
SEBS 92 1 TiO_2-NH_2	1.9 ± 0.3	26 ± 15	23.0 ± 0.4
SEBS 92 1 TiO_2-SO_3H	2.4 ± 0.4	52 ± 25	37.0 ± 0.5

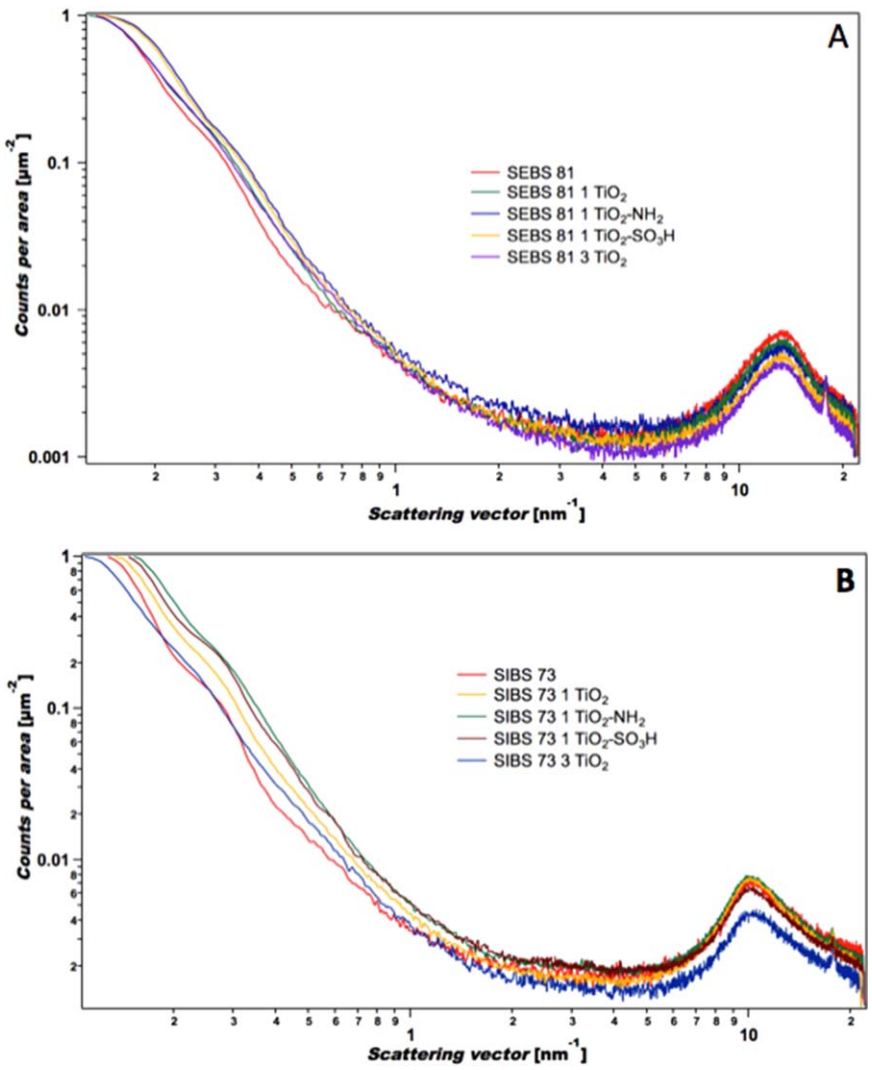

Figure 7. SAXS patterns: (A) SEBS 81 and (B) SIBS 73. [Color figure can be viewed in the online issue, which is available at wileyonlinelibrary.com.]

Table III. SAXS Distances

Membrane	Interstitial Distance 1 (nm)	Interstitial Distance 2 (nm)
SEBS 0	31.7	0.46
SEBS 81	46.8	0.47
SEBS 81 1 TiO_2	49.1	0.46
SEBS 81 1 TiO_2-NH_2	44.7	0.49
SEBS 81 1 TiO_2-SO_3H	46.8	0.48
SEBS 81 3 TiO_2	46.8	0.50
SEBS 92	50.7	0.46
SEBS 92 1 TiO_2	44.7	0.46
SEBS 92 1 TiO_2-NH_2	51.7	0.46
SEBS 92 1 TiO_2-SO_3H	49.1	0.49
SEBS 92 3 TiO_2	44.7	0.46
SIBS 0	31.7	0.61
SIBS 73	49.1	0.58
SIBS 73 1 TiO_2	46.8	0.61
SIBS 73 1 TiO_2-NH_2	40.9	0.61
SIBS 73 1 TiO_2-SO_3H	42.7	0.61
SIBS 73 3 TiO_2	57.8	0.60
SIBS 82	42.7	0.61
SIBS 82 1 TiO_2	44.6	0.61
SIBS 82 1 TiO_2-NH_2	46.8	0.62
SIBS 82 1 TiO_2-SO_3H	49.1	0.63
SIBS 82 3 TiO_2	44.7	0.62

capacity of these block copolymer is determined by the elastomeric block.[31] Similar behavior has been observed with titania incorporated to other polymers like Nafion®.[20] This could also be an explanation for the absence of chemical interactions between the functionalized nanoparticles and the sulfonic groups.

Small Angle X-ray Scattering

SAXS measurements were performed to evaluate the differences in morphology caused by sulfonation and the incorporation of nanoparticles. Sulfonation changes the morphology of the block copolymers from spherical morphology at low sulfonation levels, to lamellar structures for high sulfonation levels.[32] This study on SIBS by Elabd and coworkers, concluded that depending on the direction in which samples are analyzed (in the plane or normal to the plane of the membrane), the morphology of a sample could be inferred. In this study measurements were made normal to the plane of the membrane, and comparing the obtained SAXS patterns with one presented by Elabd[32] it can be suggested that the morphology of both of these highly sulfonated polymers is lamellar given that in this direction no morphological features can clearly be seen.

The incorporation of nanoparticles into the highly sulfonated polymers produces small changes in the slope and the form of the scattering curve [Figure 7(A,B)]. However, the changes in the interstitial distances, calculated using Bragg's law, were significant, as presented on Table III. Changes are unique for each type and loading of titania and for each polymer and sulfonation level. However, the fact that there are changes ranging from 2 to 7 nm could explain the changes in properties of the membranes. Although it is suggested that there are no interactions between nanoparticles and ionic domains, the presence of the nanoparticles has some effect on the arrangement of the different blocks in the polymers and, as a result, on their transport properties.

Wide Angle X-ray Scattering

WAXS results show diffraction patterns for the titania nanoparticles used, that coincide with the angles of the X-ray diffraction (XRD) pattern of the anatase titanium dioxide crystal structure[33] (Figure 8) confirming the type of particles used. Even after being incorporated into the membranes and after functionalization, the angle of the peaks does not change. Thus, suggesting that there are poor or no interactions with the polymer

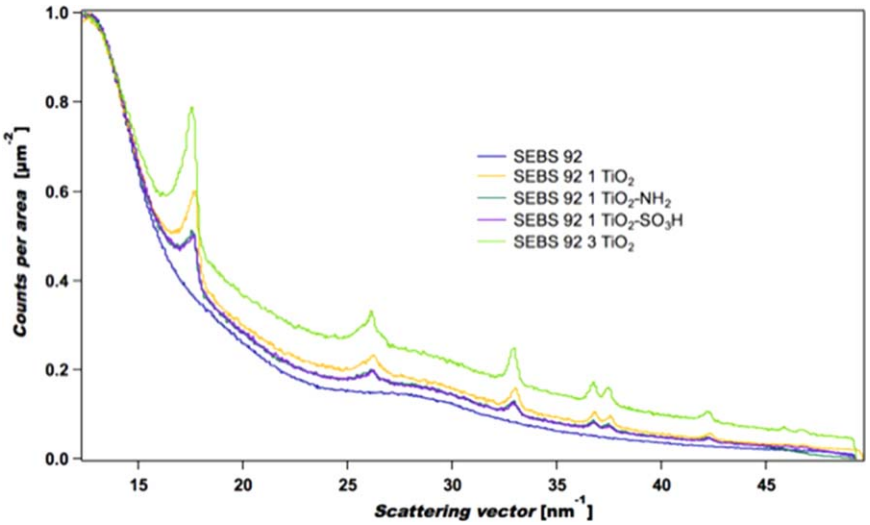

Figure 8. WAXS pattern SEBS 92. [Color figure can be viewed in the online issue, which is available at wileyonlinelibrary.com.]

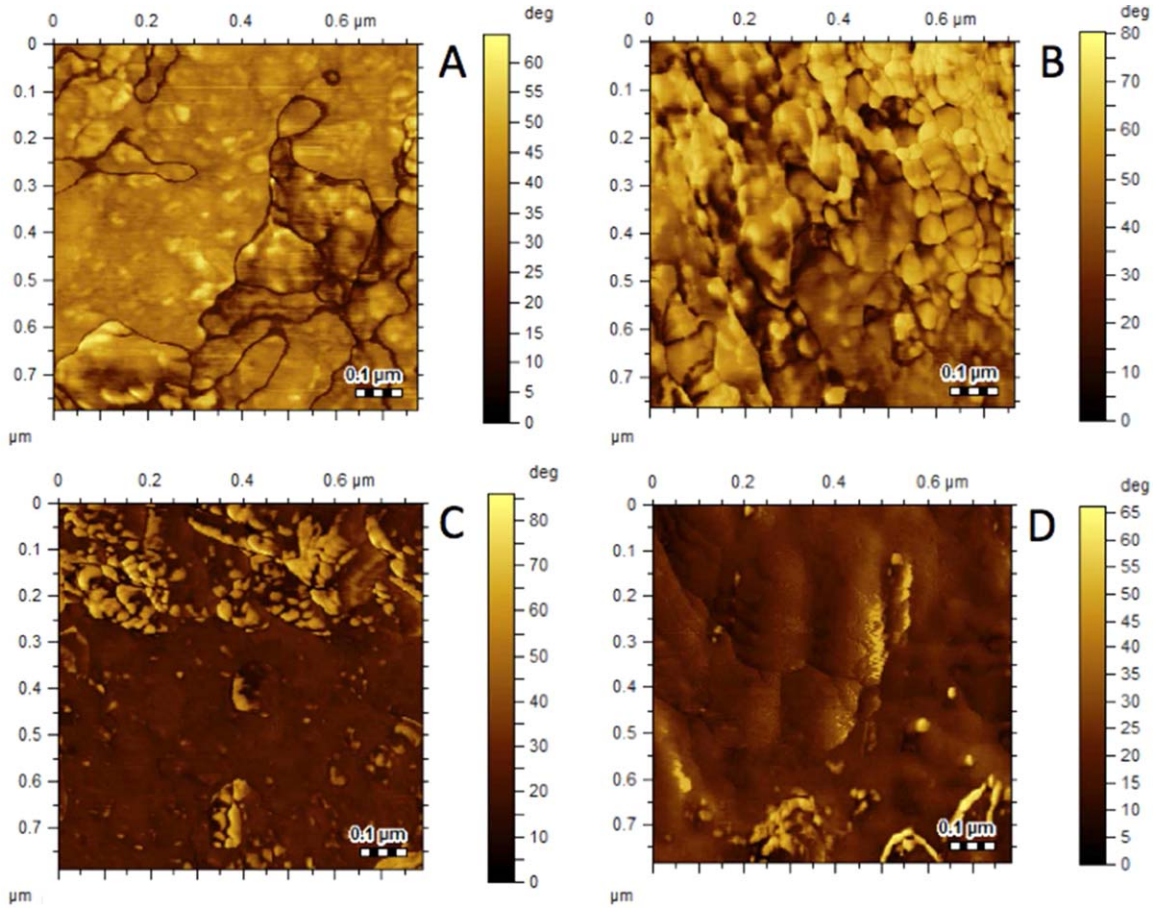

Figure 9. Phase images of SIBS 82 1 TiO2 (A) top side, (B) titania side and SIBS 82 1 TiO_2–NH_2 (C) top side, (D) titania side. [Color figure can be viewed in the online issue, which is available at wileyonlinelibrary.com.]

even though the distances and the morphology of the polymer appear to be affected by TiO_2, as suggested by SAXS results. These WAXS results contrast with other study found in the literature, where the angles in the diffraction pattern change due to polymer-filler interactions.[4] Contrasting also with SAXS results, differences in WAXS patterns due to sulfonation are not observed, suggesting that at the smallest scales there are no changes on the polymer structure caused by sulfonation.

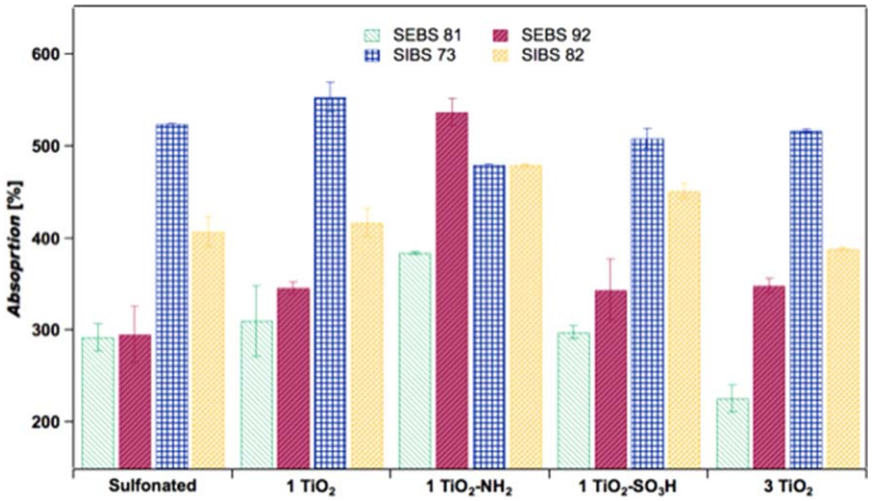

Figure 10. Effect of elastomer, sulfonation level, particle loading, and functionalization on water absorption. [Color figure can be viewed in the online issue, which is available at wileyonlinelibrary.com.]

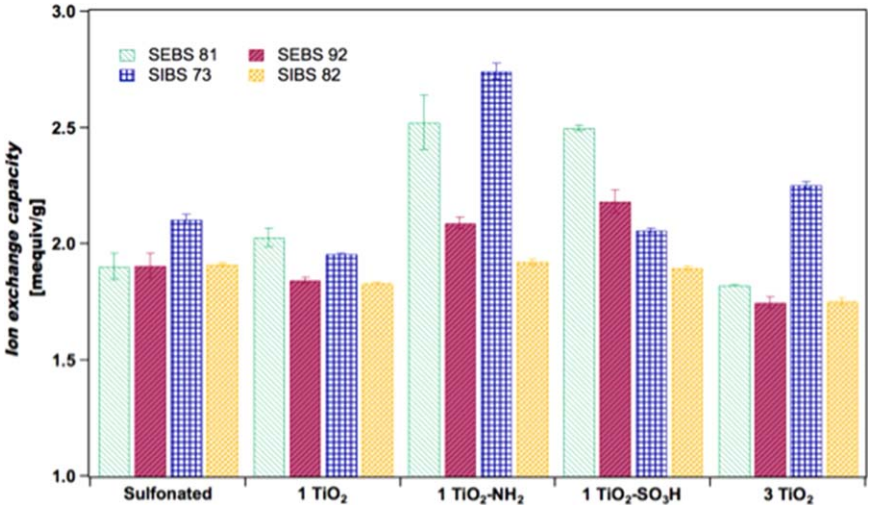

Figure 11. Effect of elastomer, sulfonation level, particle loading, and functionalization on IEC. [Color figure can be viewed in the online issue, which is available at wileyonlinelibrary.com.]

Atomic Force Microscopy (AFM)

AFM was used in the intermittent contact mode, also known as AC mode, for a qualitative determination of the agglomeration of the nanoparticles in the polymer. In this case the phase image is presented to illustrate the two phases formed when titanium dioxide modified membranes are casted. Figure 9(A) corresponds to the upper phase of the membrane SIBS 82 1 TiO_2. From the figure, it can be inferred that there are no nanoparticles on the surface; however, there seem to be nanoparticles directly under the surface that can be detected by the microscope. Figure 9(B) belongs to the bottom of the same membrane, which is rich in titania. The clusters of nanoparticles can be clearly observed on the image. The membrane with the same sulfonation level, but with amino functionalized nanoparticles (SIBS 82 1 TiO_2-NH_2) was also characterized using AFM [Figure 9(C,D)]. Results agree with the ones obtained with FT-IR, and demonstrate that the particles are more homogeneously distributed when they are functionalized. No agglomerations are observed, and images for the lower and upper side of the membrane are similar. Similar images were obtained for all the membranes studied.

Water Absorption

As previously mentioned, membranes should be hydrated to be able to properly transport protons. Previous communications have shown that water absorption increases with sulfonation levels and IEC.[11,30] It can be observed from Figure 10 that although the sulfonation percents obtained with SEBS are higher than those obtained with SIBS, the amount of water absorbed by SEBS is lower than the amount absorbed by SIBS membranes. These results suggest that there are different types of water on the membrane and that not all the sulfonic groups are available for water absorption. In terms of the effect of titania nanoparticles on this property, it can be observed that the addition of a small amount of particles (1 wt %) increases the absorption of water. When 3 wt % of TiO_2 nanoparticles were added to the polymer, the water absorption was reduced or remained constant. With these results, it could be suggested

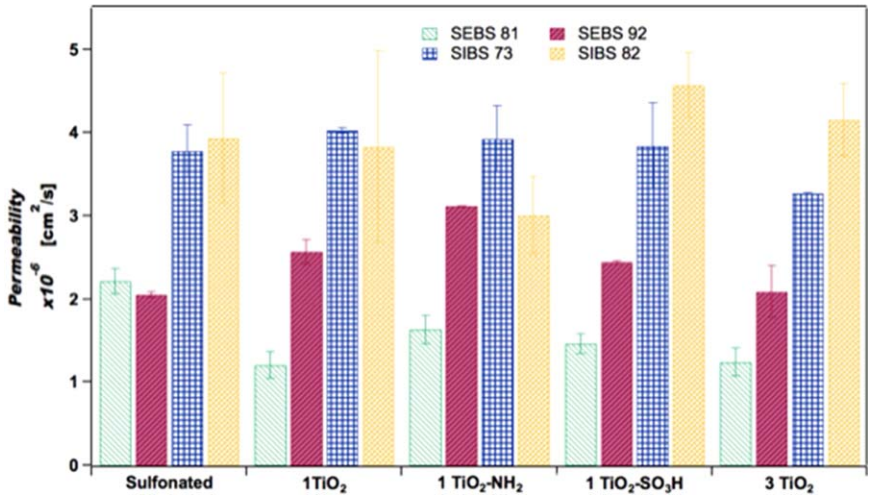

Figure 12. Effect of elastomer, sulfonation level, particle loading, and functionalization on methanol permeability. [Color figure can be viewed in the online issue, which is available at wileyonlinelibrary.com.]

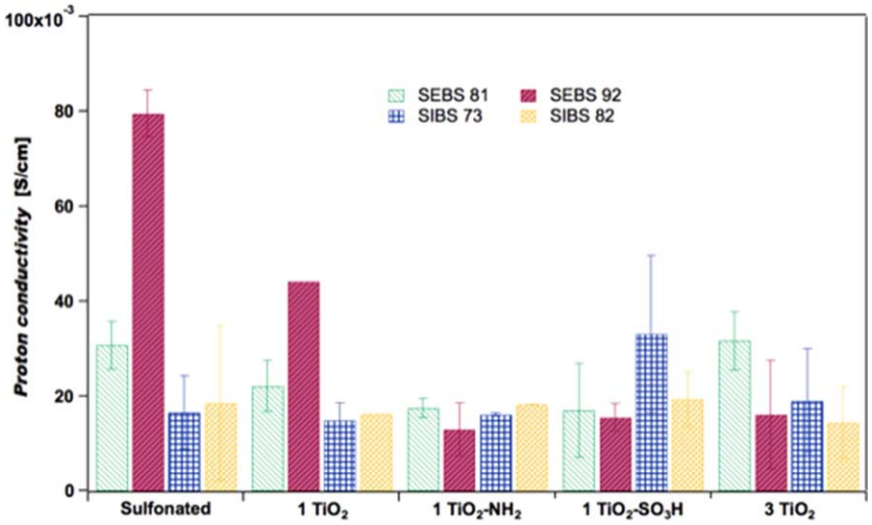

Figure 13. Effect of elastomer, sulfonation level, particle loading, and functionalization on proton conductivity. [Color figure can be viewed in the online issue, which is available at wileyonlinelibrary.com.]

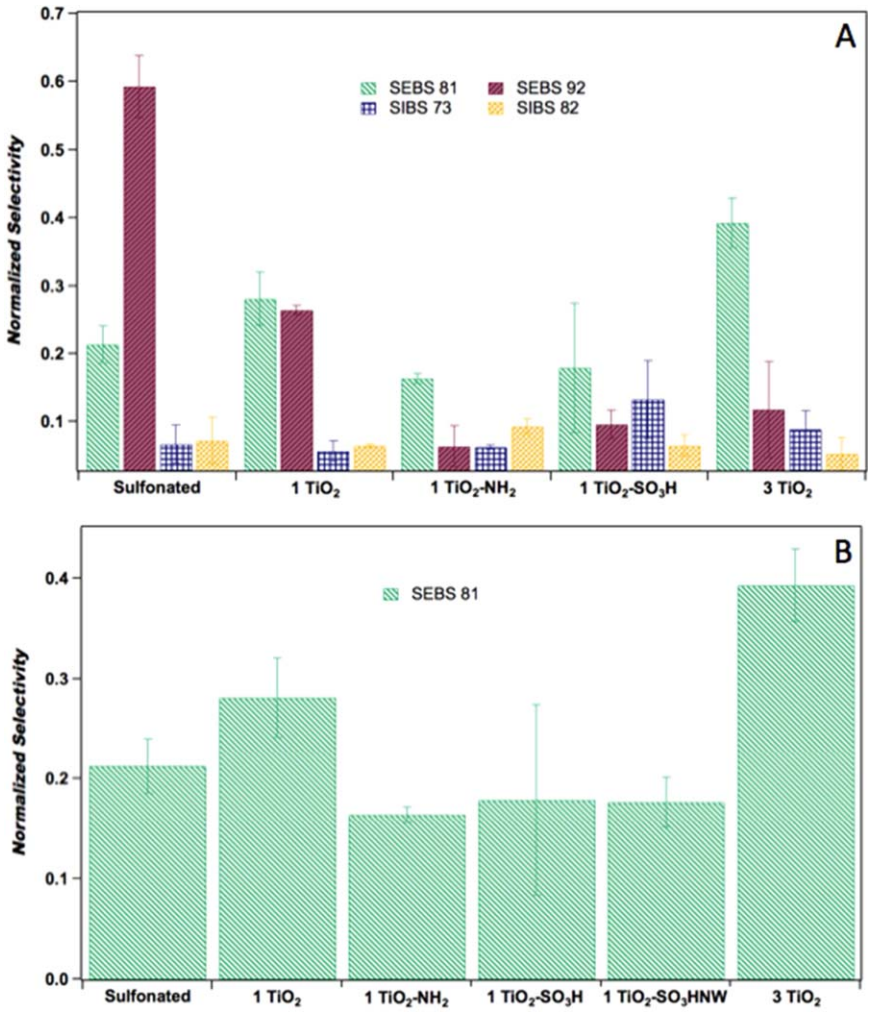

Figure 14. Normalized selectivity: (A) summary and (B) comparison between nanotubes and nanowires. [Color figure can be viewed in the online issue, which is available at wileyonlinelibrary.com.]

Table IV. Membranes Properties

Sample	Water absorption [%]	Ion exchange capacity [mequiv/g]	Methanol permeability (10^6) [cm^2/s]	Proton conductivity [S/cm]	Normalized selectivity
SEBS 81	290 ± 10	1.91 ± 0.06	2.2 ± 0.1	0.031 ± 0.005	0.21 ± 0.03
SEBS 81 1 TiO_2	310 ± 40	2.03 ± 0.04	1.2 ± 0.2	0.022 ± 0.005	0.28 ± 0.04
SEBS 81 1 TiO_2-NH_2	384 ± 1	2.5 ± 0.1	1.6 ± 0.2	0.017 ± 0.002	0.164 ± 0.007
SEBS 81 1 TiO_2-SO_3H	298 ± 7	2.50 ± 0.01	1.5 ± 0.1	0.02 ± 0.01	0.18 ± 0.09
SEBS 81 3 TiO_2	230 ± 10	1.827 ± 0.004	1.2 ± 0.2	0.032 ± 0.006	0.39 ± 0.04
SEBS 92	300 ± 30	1.91 ± 0.05	2.06 ± 0.04	0.080 ± 0.005	0.59 ± 0.05
SEBS 92 1 TiO_2	347 ± 6	1.85 ± 0.01	2.6 ± 0.1	0.044 ± 0	0.264 ± 0.007
SEBS 92 1 TiO_2-NH_2	540 ± 10	2.09 ± 0.02	3.12 ± 0	0.013 ± 0.006	0.06 ± 0.03
SEBS 92 1 TiO_2-SO_3H	340 ± 30	2.18 ± 0.05	2.45 ± 0.02	0.015 ± 0.003	0.09 ± 0.02
SEBS 92 3 TiO_2	349 ± 7	1.75 ± 0.03	2.1 ± 0.3	0.02 ± 0.01	0.12 ± 0.07
SIBS 73	524.6 ± 0.6	2.11 ± 0.02	3.8 ± 0.3	0.017 ± 0.008	0.07 ± 0.03
SIBS 73 1 TiO_2	550 ± 20	1.96 ± 0.02	4.03 ± 0.04	0.015 ± 0.004	0.06 ± 0.02
SIBS 73 1 TiO_2-NH_2	480.2 ± 0.4	2.74 ± 0.03	3.9 ± 0.4	0.0162 ± 0.0004	0.063 ± 0.003
SIBS 73 1 TiO_2-SO_3H	510 ± 10	2.061 ± 0.009	3.8 ± 0.5	0.03 ± 0.02	0.13 ± 0.06
SIBS 73 3 TiO_2	518 ± 1	2.26 ± 0.01	3.270 ± 0.007	0.02 ± 0.01	0.09 ± 0.03
SIBS 82	410 ± 20	1.914 ± 0.007	3.9 ± 0.8	0.02 ± 0.02	0.07 ± 0.03
SIBS 82 1 TiO_2	420 ± 20	1.834 ± 0.004	3 ± 1	0.02 ± 0	0.065 ± 0.002
SIBS 82 1 TiO_2-NH_2	480 ± 2	1.92 ± 0.01	3.0 ± 0.5	0.01823± 0.00007	0.09 ± 0.01
SIBS 82 1 TiO_2-SO_3H	451 ± 8	1.90 ± 0.01	4.6 ± 0.4	0.019 ± 0.006	0.06 ± 0.02
SIBS 82 3 TiO_2	389 ± 2	1.76 ± 0.02	4.2 ± 0.4	0.014 ± 0.008	0.05 ± 0.02

that high concentrations of particles can block and occupy spaces that were previously occupied by water molecules. Membranes with sulfonated nanoparticles showed almost the same water absorption as the membranes with 1% of unmodified particles. The greatest increment in water absorption was observed for the amino functionalized nanoparticles and it could imply that these membranes provide the best results. In all cases the lowest water absorption was obtained with SEBS 81, and the highest values corresponded to SIBS 73.

Ion Exchange Capacity (IEC)

Figure 11 shows that TiO_2 has different effects on the IEC of the different polymers studied. For SIBS 82 there appears to be no significant effect, other than a slight increment when functionalized nanoparticles are incorporated. SEBS 92 demonstrated a similar behavior. For the other polymers (SEBS 81 and SIBS 73) the incorporation of functionalized nanoparticles produced higher IEC values. Because all sulfonation levels are high and similar, the IEC is also similar for all the membranes and does not appear to be directly related to the amount of water. It is then suggested that not all types of water are good in transport properties and that not all sulfonic groups are active sites for proton transport. The highest variation in IEC is obtained with the incorporation of functionalized nanoparticles, especially for SEBS. A membrane with a balance between water absorption and IEC should be a good alternative as PEM.

Methanol Permeability

Figure 12 shows the significant difference in methanol permeability between SIBS and SEBS. High permeabilities, in some cases two times higher than SEBS, are obtained with SIBS membranes.[11] On the contrary, all SEBS membranes show low permeabilities that compare to the value obtained at the same conditions for the standard Nafion® 117. In this case, it can be inferred that the elastomeric block polyethylene/polybutylene has better properties for blocking the transport of methanol through the membrane than polyisobutylene. Permeabilities are very similar for almost all membranes after incorporation of functionalized and unfunctionalized TiO_2 nanoparticles. The highest reduction in permeability is observed for SEBS 81 membranes after the incorporation of the nanoparticles. These results suggest that the overall effect of the incorporation of titania nanoparticles is to maintain or reduce the methanol permeability, probably by reducing the free volume inside the membrane.

Proton Conductivity

Proton conductivities increase with sulfonation level,[11,32] as observed in Figure 13. Upon the incorporation of titania nanoparticles the proton conductivity decreases. In some cases a slight increment in conductivity is obtained with the incorporation of sulfonated nanoparticles, but the conductivity is still low, demonstrating that the transport of protons is dependent on membranes hydration and the availability of the ionic groups for interaction. With the incorporation of the

nanoparticles some agglomerations are formed, blocking the path for protons through the membranes. The number and interconnections of the ionic domains influence the proton conductivity, which could be related to the types of water present and the morphology. Although the incorporation of nanoparticles maintained or increased the water absorption of the membranes (Figure 10), not necessarily the conductivity was positively affected by this important factor. This could be explained by a lack of interconnection between the ionic domains causing the water to be in places where conductivity could not be promoted. Moreover, at the operating temperatures of the cell (80°C) these membranes dehydrate, causing a reduction in proton conductivity, showing that the nanoparticles did not help in the enhancement of the water retention ability of the polymers. When compared to the state-of-the-art Nafion® at the same experimental conditions (0.0779 S/cm) the conductivities of the studied membranes are in the same order of magnitude and one of the membranes, SEBS 92, has a similar conductivity (0.0798 S/cm). Confirming that with these polymers properties similar to the commercial PEMs can be obtained.

Normalized Selectivity

Because transport of species through this type of materials depends on different properties, it is expected that the effect of the particles on each membrane would be different, given that the polymers show differences in all their properties. In a previous study it was suggested that for sulfonated SIBS there was an optimum level of sulfonation around 84 percent.[11] In the case of SEBS, even with two sulfonation levels, it appears that there is an optimum sulfonation level at 92%. As observed along this study, SEBS presents better thermal, mechanical, and transport properties than SIBS, making it more suitable for DMFC applications. It is confirmed with the selectivity values [Figure 14(A)] obtained. The highest selectivity was obtained with SEBS 92. However, when nanoparticles are incorporated into the polymer matrix the selectivity is significantly reduced mainly due to the formation of agglomerations and the absence of interconnection between the ionic domains. SEBS 81 showed better selectivity values after the incorporation of nanoparticles demonstrating again that the effect is different for each material. PNM properties are summarized in Table IV.

To finalize the study, a different type of nanostructure, TiO_2 nanowires (NW), was evaluated. SEBS 81 was casted with TiO_2 NW, with the same amount (1 wt %) and sulfonation functionalization as the nanoparticles, and the results for normalized selectivity are compared with the other SEBS 81 membranes [Figure 14(B)]. The effect of this type of nanostructure does not seem to be very significant on this polymer given that contrasting with the literature the value of selectivity is similar to the value obtained with sulfonated nanoparticles.

CONCLUSIONS

Two sulfonated block copolymer ionomers (SEBS and SIBS), used as PEMs for DMFC applications, showed significant differences in their thermal, mechanical, and transport properties. The blocking ability of the elastomer for methanol is more effective for polyethylene/polybutylene than for polyisobutylene, and it is also the most stable elastomer. The incorporation of TiO_2 nanoparticles into these polymer membranes showed that unfunctionalized nanoparticles tend to agglomerate and form two phases on the membrane. Functionalization of the nanoparticles seemed to enhance the dispersion of the particles on the polymer matrix, creating more homogeneous membranes and affecting the transport, mechanical, and morphological properties. Functionalized nanoparticles maintained or reduced the permeation of methanol through the PNM. Unfortunately, they also reduced the transport of protons through the PNM, possibly due to poor interconnection of the ionic domains throughout the membrane. This was the case, even though there were significant variations in the amount of water absorbed and IEC with the different loadings and functionalizations. Of the functionalized nanoparticles studied, sulfonated nanoparticles seemed to have slightly better selectivity than amino functionalized nanoparticles. The best selectivity results after comparison with the state-of-the-art Nafion® were obtained with SEBS 92. A comparison of the selectivities of the membranes with sulfonated nanoparticles and nanowires showed no significant difference among the particle's shape.

ACKNOWLEDGMENTS

This research was possible thanks to the financial support of the NSF CREST through grants number HDR-0833112 and HDR-1345156. Financial support by the U.S, Army Research Laboratory and the U.S. Army Research Office under contract/grants numbers W911NF1410076 (SAXS facilities) and W911NF1310166 (AFM equipment) is also acknowledged. The authors acknowledge the help and support of Stephany Herrera with the DSC and the rheometer experiments and the laboratory of Dr. Marco De Jesus for the Raman experiments. Finally, the assistance of the undergraduate students: Michelle Marrero, Marialejandra González, Nelson Rodríguez, Vanessa Torres, and Edwin Torres is also greatly appreciated.

REFERENCES

1. Tripathi, B. P.; Shahi, V. K. *Prog. Polym. Sci.* **2011**, *36*, 945.
2. Kim, B.; Kim, J.; Cha, B. J.; Jung, B. *J. Membr. Sci.* **2006**, *280*, 270.
3. Beydaghi, H.; Javanbakht, M.; Salar Amoli, H.; Badiei, A.; Khaniani, Y.; Ganjali, M. R.; Norouzi, P.; Abdouss, M. *Int. J. Hydrogen Energy* **2011**, *36*, 13310.
4. Unnikrishnan, L.; Mohanty, S.; Nayak, S. K.; Jayan, N. P. *Int. J. Plast. Technol.* **2011**, *15*, 1.
5. De Bonis, C.; Cozzi, D.; Mecheri, B.; D'Epifanio, A.; Rainer, A.; De Porcellinis, D.; Licoccia, S. *Electrochim. Acta* **2014**, *147*, 418.
6. Lin, Y.-F.; Yen, C.-Y.; Ma, C.-C. M.; Liao, S.-H.; Lee, C.-H.; Hsiao, Y.-H.; Lin, H.-P. *J. Power Sources* **2007**, *171*, 388.
7. Di Vona, M. L.; Ahmed, Z.; Bellitto, S.; Lenci, A.; Traversa, E.; Licoccia, S. *J. Membr. Sci.* **2007**, *296*, 156.
8. Di Vona, M. L.; Sgreccia, E.; Donnadio, A.; Casciola, M.; Chailan, J. F.; Auer, G.; Knauth, P. *J. Membr. Sci.* **2011**, *369*, 536.

9. Shahi, V. K. *Solid State Ionics* **2007**, *177*, 3395.
10. Mistry, M. K.; Choudhury, N. R.; Dutta, N. K.; Knott, R. *J. Membr. Sci.* **2010**, *351*, 168.
11. Avilés-Barreto, S. L.; Suleiman, D. *J. Appl. Polym. Sci.* **2013**, *129*, 2294.
12. Mauritz, K. a.; Blackwell, R. I.; Beyer, F. L. *Polymer* **2004**, *45*, 3001.
13. Zhao, J.; Milanova, M.; Warmoeskerken, M. M. C. G.; Dutschk, V. *Colloid. Surf. A Physicochem. Eng. Asp.* **2012**, *413*, 273.
14. Jian-hua, T.; Peng-fei, G.; Zhi-yuan, Z.; Wen-hui, L.; Zhong-qiang, S. *Int. J. Hydrogen Energy* **2008**, *33*, 5686.
15. Zhengbang, W.; Tang, H.; Mu, P. *J. Membr. Sci.* **2011**, *369*, 250.
16. Wang, L. S.; Xiao, M. W.; Huang, X. J.; Wu, Y. D. *J. Hazard. Mater.* **2009**, *161*, 49.
17. Matos, B. R.; Santiago, E. I.; Rey, J. F. Q.; Ferlauto, a. S.; Traversa, E.; Linardi, M.; Fonseca, F. C. *J. Power Sources* **2011**, *196*, 1061.
18. Jun, Y.; Zarrin, H.; Fowler, M.; Chen, Z. *Int. J. Hydrogen Energy* **2011**, *36*, 6073.
19. Xu, T.; Hou, W.; Shen, X.; Wu, H.; Li, X.; Wang, J.; Jiang, Z. *J. Power Sources* **2011**, *196*, 4934.
20. Li, Q.; Zhang, H.; Tu, Z.; Yu, J.; Xiong, C.; Pan, M. *J. Membr. Sci.* **2012**, *423–424*, 284.
21. Suleiman, D.; Carreras, G.; Soto, Y. *J. Appl. Polym. Sci.* **2013**, *128*, 2297.
22. Elabd, Y. A.; Napadensky, E. *Polymer* **2004**, *45*, 3037.
23. Razmjou, A.; Resosudarmo, A.; Holmes, R. L.; Li, H.; Mansouri, J.; Chen, V. *Desalination* **2012**, *287*, 271.
24. Liu, Z.; Guo, B.; Huang, J.; Hong, L.; Han, M.; Gan, L. M. *J. Power Sources* **2006**, *157*, 207.
25. Martinez-Felipe, A.; Imrie, C. T.; Ribes-Greus, A. *J. Appl. Polym. Sci.* **2013**, *127*, 246.
26. Barreto, S. M. A.; Suleiman, D. *J. Membr. Sci.* **2010**, *362*, 471.
27. Smitha, B. *J. Membr. Sci.* **2003**, *225*, 63.
28. Cozzi, D.; De Bonis, C.; D'Epifanio, A.; Mecheri, B.; Tavares, A. C.; Licoccia, S. *J. Power Sources* **2014**, *248*, 1127.
29. Suleiman, D.; Napadensky, E.; Sloan, J. M.; Crawford, D. M. *Thermochim. Acta* **2007**, *460*, 35.
30. Suleiman, D.; Padovani, A. M.; Negrón, A. A.; Sloan, J. M.; Napadensky, E.; Crawford, D. M. *J. Appl. Polym. Sci.* **2014**, *40344*, 1.
31. Storey, R. F.; Chisholm, B. J.; Lee, Y. *Polym. Eng. Sci.* **1997**, *37*, 73.
32. Elabd, Y. A.; Walker, C. W.; Beyer, F. L. *J. Membr. Sci.* **2004**, *231*, 181.
33. Qiu, Y.; Yu, J. *Solid State Commun.* **2008**, *148*, 556.